HHS Public Access

Author manuscript

Mol Psychiatry. Author manuscript; available in PMC 2015 August 01.

Published in final edited form as:

Mol Psychiatry. 2015 February ; 20(2): 215–223. doi:10.1038/mp.2013.192.

FGF-21, a novel metabolic regulator, has a robust neuroprotective role and is dramatically elevated in neurons by mood stabilizers

Yan Leng, M.D.[1], **Zhifei Wang, Ph.D.**[1], **Li-Kai Tsai, M.D., Ph.D**[1], **Peter Leeds, B.S.**[1], **Emily Bame Fessler, B.S.**[1], **Junyu Wang, B.S.**[1], and **De-Maw Chuang, Ph.D.**[1]

[1]Section on Molecular Neurobiology, National Institute of Mental Health, National Institutes of Health, Bethesda, MD, 20892-1363

Abstract

Fibroblast growth factor-21 (FGF-21) is a new member of the FGF super-family and an important endogenous regulator of glucose and lipid metabolism. It has been proposed as a therapeutic target for diabetes and obesity. Its function in the central nervous system (CNS) remains unknown. Previous studies from our laboratory demonstrated that aging primary neurons are more vulnerable to glutamate-induced excitotoxicity, and that co-treatment with the mood stabilizers lithium and valproic acid (VPA) induces synergistic neuroprotective effects. This study sought to identify molecule(s) involved in these synergistic effects. We found that FGF-21 mRNA was selectively and dramatically elevated by co-treatment with lithium and VPA in primary rat brain neurons. FGF-21 protein levels were also robustly increased in neuronal lysates and culture medium following lithium-VPA co-treatment. Combining glycogen synthase kinase-3 (GSK-3) inhibitors with VPA or histone deacetylase (HDAC) inhibitors with lithium synergistically increased FGF-21 mRNA levels, supporting that synergistic effects of lithium and VPA are mediated via GSK-3 and HDAC inhibition, respectively. Exogenous FGF-21 protein completely protected aging neurons from glutamate challenge. This neuroprotection was associated with enhanced Akt-1 activation and GSK-3 inhibition. Lithium-VPA co-treatment dramatically prolonged lithium-induced Akt-1 activation and augmented GSK-3 inhibition. Akt-1 knockdown markedly decreased FGF-21 mRNA levels, and reduced the neuroprotection induced by FGF-21 or lithium-VPA co-treatment. In addition, FGF-21 knockdown reduced lithium-VPA co-treatment-induced Akt-1 activation and neuroprotection against excitotoxicity. Together, our novel results suggest that FGF-21 is a key mediator of the effects of these mood stabilizers, and a potential new therapeutic target for CNS disorders.

[1]Correspondence: Dr. De-Maw Chuang, Section on Molecular Neurobiology, National Institute of Mental Health, National Institutes of Health, 10 Center Dr., MSC-1363, Bethesda, MD, 20892-1363. Phone: (301) 496-4915. Fax: (301) 480-9290. chuang@mail.nih.gov.

CONFLICT OF INTEREST

All authors have no conflict of interest to disclose, financial or otherwise.

Keywords

FGF-21; GSK-3 inhibitor; HDAC inhibitor; lithium; valproic acid; neuroprotection

INTRODUCTION

Fibroblast growth factor-21 (FGF-21) is a recently discovered metabolic regulator shown to facilitate glucose and lipid metabolism[1]. When administered systemically to obese, insulin resistant rodents and diabetic monkeys, FGF-21 enhances energy utilization, improves insulin sensitivity and induces weight loss[2–6]. By interacting with its specific cell surface receptors and its co-receptor β-Klotho, FGF-21 also regulates the expression of genes involved in gluconeogenesis, lipogenesis, lipolysis, and fatty acid oxidation[3, 7, 8]. During fasting, FGF-21 is induced in the liver, the major site of its production, by mechanisms involving the activation of the nuclear receptor peroxisome proliferator-activated receptor α; (PPARα)[1, 9]. In addition, FGF-21 is upregulated in adipose tissue through PPARγ[10], and controls PPARγ activity in an autocrine manner to enhance adipogenesis and to mediate the clinical and side effects of PPARγ agonists thiazolidinediones[11]. In clinical studies, higher serum levels of FGF-21 were found in patients with metabolic disorders such as type 2 diabetes, fatty liver disease, and coronary artery disease[12–14]. This suggests that these metabolic disorders involve FGF-21 resistance or compensatory response to specific metabolic stress. Interestingly, intracerebral ventricular injection of human recombinant FGF-21 in rats increases hepatic insulin sensitivity and metabolic rate in diet-induced obesity[15]. These results suggest that the central nervous system (CNS) is likely a significant target for the potential benefits of FGF-21 in the treatment of diabetes and obesity.

Emerging evidence suggests that FGF-21 has some protective effects. For example, FGF-21 has been shown to improve the survival and function of pancreatic β-cells by activating protein kinase B (Akt) and extracellular signal related kinase (ERK) 44/42 signaling pathways[16], protect animals from the adverse effects of lipopolysaccharide and sepsis[17] as well as against cardiac hypertrophy[18], and prevent palmitate-induced insulin resistance by inhibiting the activation of stress kinase and NF-κB[19]. Autophagy deficiency and the resultant mitochondrial dysfunction have also been reported to enhance FGF-21 expression and collectively protect against diet-induced obesity and insulin resistance[20]. However, whether FGF-21 is expressed in brain neurons, or exhibits specific functions such as neuroprotection, remains unknown.

Recent studies have observed that mood stabilizing drugs used to treat bipolar disorder, notably lithium and valproic acid (VPA), have neuroprotective properties against multiple insults in both *in vivo* and *in vitro* experimental settings as well as in clinical studies. By inhibiting glycogen synthase kinase-3 (GSK-3), lithium modulates transcriptional regulation of genes involved in neuroprotection and neurotrophism such as B-cell lymphoma 2 (Bcl-2), p53, Bcl-2 associated X protein (Bax) and brain-derived neurotrophic factor (BDNF)[21, 22]. On the other hand, VPA has been identified as a pan inhibitor of histone deacetylases (HDACs)[23, 24]. Via HDAC inhibition, VPA remodels chromatin structure to activate transcriptional factors, thereby inducing prominent molecules, including heat-shock

protein-70 (HSP70), Bcl-2, α-synuclein, BDNF, and vascular endothelial growth factor (VEGF)[21, 25, 26]. In primary young cultures of brain neurons including cerebellar granular cells (CGCs), pretreatment with either lithium or VPA robustly protects against glutamate-induced, N-methyl D-aspartate (NMDA) receptor-mediated excitotoxicity[27, 28]. Interestingly, in aging CGCs, treatment with either lithium or VPA alone produces only marginal neuroprotection against excitotoxicity; in contrast, combined treatment with these two drugs induces synergistic neuroprotective effects[28].

The synergic neuroprotective effects of lithium-VPA co-treatment are associated with enhancement of GSK-3 inhibition induced by lithium alone[28]. However, the gene whose expression is critical for the neuroprotective synergy remains unidentified. In this study, we used mRNA microarray and quantitative PCR to demonstrate for the first time that FGF-21 is robustly induced by co-treatment with the mood stabilizers lithium and VPA. Further, we show that FGF-21 plays a remarkable neuroprotective role via mechanisms involving Akt-1 activation and is part of the molecular complex underlying the synergistic neuroprotection induced by mood stabilizers. In addition, our results suggest that FGF-21 is a potential new target for the treatment of brain disorders.

METHODS

Primary rat CGC, hippocampal, and cerebral cortical neuronal cultures

Eight-day-old Sprague-Dawley rats were used to prepare CGCs as previously described[28], and according to procedures approved by the NIH Animal Care and Use Committee. Dissociated cells were resuspended in 2% serum-free Gem21 (Gemini, West Sacramento, CA, USA)/neurobasal medium (Life Technologies, Grand Island, NY, USA) and plated at a density of 1.6×10^6 cells/ml on poly-L-lysine pre-coated 96-well plates (Corning Incoporated, Corning, NY, USA), 6-well plates (BD Bioscience, Franklin Lakes, NJ, USA), or chamber slides (Nalge Nunc International, Rochester, NY, USA). Cytosine arabinofuranoside (10 μM; Arac) was added to the cultures about 24 hours after plating to arrest the growth of non-neuronal, replicating cells. The cells were maintained at 37°C in the presence of 5% CO_2/95% air in a humidified incubator. During experiments, more than 92% of cells represented neurons.

The brains of 18-day-old rat embryos were used to prepare hippocampal and cerebral cortical neuronal cells, as previously described[27, 29]. In brief, hippocampi and cortices were dissected from embryonic brain, and cells were dissociated by trypsinization and trituration, followed by DNase treatment. The dissociated cells were resuspended in 2% serum-free Gem21/neurobasal medium and plated at a density of 7×10^5 cells/ml on 6-well plates or chamber slides pre-coated with 0.01% poly-D-lysine. Five μM Arac was added to the cultures around 48 hours after plating to arrest the replication of non-neuronal cells. Hippocampal and cortical neurons were treated with lithium, VPA, or their combination for 2 days, starting at DIV-6, as specified. At DIV-6, CGCs, hippocampal and cortical neurons were stained for neuronal marker MAP2 to show their typical mature morphologies (Supplementary Fig. S1).

Animal treatments

Animal care was conducted in according to the National Institutes of Health *Guidelines for the Care and Use of Laboratory Animals*. Two-month old male CD-1 mice (20–25 g; Charles River, Wilmington, MA, USA) were grouped and housed five animals per cage with free access to food and water, and on a 12 h light/dark cycle. Mice were fed with a chow (Bio-Serv, Frenchtown, NJ, USA) containing bacon flavor alone, lithium carbonate (3 g/kg), sodium VPA (25 g/kg), or lithium carbonate-sodium VPA combination. Following dietary treatment for 28 days, mice were killed, and the brains were removed and frozen for RNA extraction. Serum concentrations of both drugs were within their therapeutic levels after chronic dietary treatment[28].

Microarray mRNA analysis

CGCs were treated with 3 mM lithium chloride, 0.8 mM VPA, or their combination at DIV-6, and then harvested 48 hours later for total RNA extraction using an RNeasy Mini Kit (Qiagen, Valencia, CA, USA). The isolated RNA (10 μg) was transcribed into double stranded cDNA using a Superscript Double-Stranded cDNA Synthesis Kit (Life Technologies), followed by sample labeling, hybridization, scan and microarray mRNA analyses (Roche Applied Science, Indianapolis, IN, USA). Microarray data were analyzed using DNASTAR ArrayStar 5 software (DNASTAR Inc., Madison, WI, USA).

Total RNA extraction and real-time quantitative polymerase chain reaction (q-PCR)

Total RNA from cells was harvested using the RNeasy® Mini-kit (Qiagen) as per the manufacturer's instructions. Each purified 2 μg RNA sample was reverse transcribed into cDNA following instructions provided by a High-Capacity cDNA Archive kit (Life Technologies). Reverse transcription (RT) reactions were performed for 10 min at 25°C, 120 min at 37°C, and 5 min at 85°C. Q-PCR was conducted with TaqMan universal PCR master mix (Life Technologies) as well as FGF-21, FGF-15, FGF-23, BDNF, GDNF, VEGF-α, PDGF-α, TGF-α, HSP70-1a, HSP70-1b, and α-synuclein gene expression assays. Negative controls without reverse transcriptase were included in each assay. PCR reactions with wells were run for 2 min at 50°C, 10 min at 95°C, and 40 cycles of 15 seconds at 95°C and 1 min at 60°C. The $2^{-\Delta\Delta Ct}$ method was used to calculate mRNA expression levels, where C_t=cycle threshold number, ΔC_t=β-actin C_t–target gene C_t, and $\Delta\Delta C_t$=ΔC_t control–ΔC_t treated cells, and mRNA level of each sample was quantified relative to matched vehicle-treated controls with β-actin as the internal reference.

ELISA

FGF-21 protein levels from the culture medium and lysates of CGCs were determined using a mouse/rat FGF-21 ELISA Kit (Aviscera Bioscience, Santa Clara, CA, USA) according to the manufacturer's protocol. Briefly, 96-well microplates pre-coated with goat anti-rabbit immunoglobulin G (IgG) were incubated overnight by adding FGF-21 antibody with samples or FGF-21 standards. After washing to remove unbound antibody and other substances, streptavidin conjugated to horseradish peroxidase was then added to the wells and incubated for 2 hours. After washing again to remove unbound enzyme, a substrate solution was added to the wells for an additional 45-min incubation followed by washing.

The enzyme reaction yielded a blue product that turned yellowish when the Stop Solution was added. The optical density of each well was detected using a microplate reader set at 450 nm, and the readings were subtracted from those at 540 nm. The intensity of the color measurement was in proportion to the amount of mouse FGF-21 bound in the initial step. Sample values were then read and calculated from the standard curve.

Measurement of cell viability

Cell viability was quantified by 3-(4,5-dimethylthiazol-2-yl)-2,5-diphenyl tetrazolium bromide (MTT) colorimetric assay for detecting mitochondrial dehydrogenase activity, as previously described[28]. Briefly, CGCs in cultures were incubated with MTT (125 μg/ml) for 2 hours at 37°C. After medium aspiration, the purple formazan product was dissolved in dimethyl sulfoxide (DMSO) and quantified spectrophotometrically at 540 nm. Cell viability results were expressed as percentage of the vehicle-treated control.

Analysis of chromatin condensation

CGCs grown on 6-well plates were washed with ice-cold PBS, fixed with ice-cold methanol for 1 min, and chromatins were stained with Hoechst dye 33258 (5 μg/ml; Sigma-Aldrich, St. Louis, MO, USA) for 3 min at 4°C as previously described[28]. Nuclei were visualized under a Zeiss Axiovert fluorescence microscope at 40× magnification.

Western blotting

CGCs were harvested in lysis buffer, followed by sonication for 30 seconds as previously described[29]. An aliquot of 10 μg of protein was dissolved in Nupage LDS sample buffer (Life Technologies), loaded into a 4–12% Nupage Bis-Tris gel (Life Technologies), and then subjected to electrophoresis. After separation, protein bands were transferred to a nitrocellulose membrane (Life Technologies), which was blocked by incubation with blocking buffer (LI-COR Biosciences, Lincoln, NE, USA) for 1 hour and further incubated overnight at 4°C with the primary antibody against GSK-3β (1:5,000; BD Bioscience), GSK-3α (1:2,000; Santa Cruz Biotechnologies, Santa Cruz, CA, USA), p-Akt-1^{Ser473}, p-GSK-3β^{Ser9}, p-ERK44/42$^{Thr202/Tyr204}$, Akt-1, ERK 44/42 (1:1,000; Cell Signaling Technology, Danvers, MA, USA), or β-actin (1:10,000; Sigma-Aldrich) in 0.1% Tween-20/PBS, and then with a secondary antibody (1:10,000; LI-COR Biosciences) labelled with a fluorescent dye. Reactive bands were scanned and analyzed by the Odyssey Infrared Imaging System (LI-COR Biosciences).

Specific mRNA knockdown using lentiviral shRNA-GSK-3β (sh-GSK-3β), shRNA-FGF-21(sh-FGF-21), and shRNA-Akt-1(sh-Akt-1)

Constructs of Mission® pLKO.1-puro control (sh-cont), sh-GSK-3β, sh-FGF-21, and sh-Akt-1 (Sigma-Aldrich) were used for gene knockdown studies. The respective shRNA sequences are shown in Table S2. Human Embryonic Kidney (HEK) 293 T/17 cells were seeded at 3×10^5 cells/well in 6-well plates with Dulbecco's Modified Eagle's medium (DMEM) and 10% fetal bovine serum (FBS). After 24 hours, cells were transfected with lentiviral shRNA constructs following the manufacturer's recommended formula [0.5 μg construct DNA, 5 μl packaging mix (Sigma-Aldrich), and 3 μl FuGENE transfection reagent

(Roche Applied Science)] in 2 ml DMEM/well. Lentiviral particles secreted into the culture medium were collected 48 hours after transfection and added onto 6- or 96-well plates immediately after CGC plating. The next day, DMEM was replaced with 2% Gem21/ neurobasal medium for gene knockdown and subsequent experiments.

Statistical analysis

Data are expressed as mean ± SEM from 3 to 4 independent experiments. Statistical significance was analysed using one-way analysis of variance (ANOVA) and Bonferroni's *post-hoc* comparison, except as specified. A p value of ≤ 0.05 was considered significant.

RESULTS

Combined lithium and VPA treatment synergistically enhances FGF-21 mRNA and protein levels in neurons

Primary neuronal cultures of CGCs from rats were treated with lithium, VPA, or their combination at day *in vitro* (DIV)-6 for 48 hours and then harvested for microarray or real-time quantitative polymerase chain reaction (q-PCR). Treatment with a combination of lithium chloride (3 mM) and VPA (0.8 mM) synergistically boosted mRNA levels of FGF-21 approximately 15-fold, as detected using the NimbleGen Gene Expression Array (Supplementary Table S1). Real time q-PCR confirmed that FGF-21 mRNA levels were moderately increased by lithium (Supplementary Fig. S2a), but not altered by VPA (Supplementary Fig. S2b); however, mRNA levels were synergistically increased by co-treatment with lithium and VPA in a time-dependent manner (Fig. 1a, b). The synergistic elevation of FGF-21 mRNA levels plateaued after 2 days of co-treatment, and lasted at least 7 days. When using ELISA, we found that FGF-21 protein in both the lysates and the culture medium was robustly elevated after combined treatment with lithium and VPA for 3 or 7 days (Fig. 1c). Potentiation of FGF-21 protein levels by lithium-VPA co-treatment for 3 or 7 days was also confirmed by Western blotting analysis (Fig. 1d).

In primary hippocampal and cortical neurons, lithium, but not VPA, also significantly increased FGF-21 mRNA levels, and more than additive increases were observed when these neurons were co-treated with lithium and VPA (Fig. 1e). In addition, FGF-21 mRNA levels in the brain of CD1 mice were significantly elevated after combined dietary treatment with lithium carbonate and sodium VPA for 28 days, while mono-treatment with either drug was ineffective (Fig. 1f). The synergistic increase in FGF-21 mRNA levels by lithium-VPA co-treatment in CGCs was highly selective among a spectrum of neurotrophic and neuroprotective proteins, including FGF-15, FGF-23, BDNF, glial cell line-derived neurotrophic factor (GDNF), VEGF-α, platelet-derived growth factor (PDGF)- α, transforming growth factor (TGF)- α, heat shock protein (HSP)70-1a, HSP70-1b and α-synuclein (α-syn) (Fig. 1g). mRNA levels of these genes were either unaffected by all treatment conditions, or modestly increased by mono-treatment with VPA, however, not synergistically by co-treatment.

We also investigated whether FGF-21 mRNA can be induced by lithium-VPA co-treatment in cells of glial origin. For this study, we employed rat C6 glioma and primary cerebral

cortical glial cells, which displayed their typical cell morphologies (Supplementary Fig. S3a). Treatment of C6 cells with 1 mM VPA in conjunction with various concentrations of LiCl resulted in a dose-dependent increase in FGF-21 mRNA levels (Supplementary Fig. S3b). A similar extent (8-fold) of the increase in FGF-21 mRNA was observed in rat primary cortical glial cultures (Supplementary Fig. S3b).

Synergistic expression of FGF-21 mRNA by lithium and VPA is mediated through GSK-3 and HDAC inhibition, respectively

By themselves, the GSK-3 inhibitors SB415286 (SB415) and SB216763 (SB216) had modest effects on FGF-21 mRNA levels in a concentration-dependent manner (Supplementary Fig. S5a). When used with VPA, 10 μM of SB415 mimicked the ability of lithium to cause synergistic increases in FGF-21 mRNA levels (Fig. 2a). Interestingly, SB415 and lithium co-treatment also markedly increased FGF-21 mRNA levels; the largest increase (approximately 40-fold) was observed when SB415, lithium, and VPA were all present (Fig. 2a). To further explore the role of GSK-3 inhibition, CGCs were transduced with lentivirus-driven GSK-3β shRNA (sh-GSK-3β) or with scramble control small hairpin RNA (shRNA; sh-cont) immediately after cell plating; the listed shRNA sequence of the studied gene is shown in Supplementary Table S2. At DIV-6, cells were harvested for Western blotting to detect total GSK-3β protein levels, or alternately, treated with lithium, VPA, or their combination for 2 days before harvesting. In keeping with our previous findings[30] sh-GSK-3β (#614) robustly reduced GSK-3β protein levels compared with the sh-cont (Fig. 2b). More importantly, after knockdown of the GSK-3β gene, an approximately 6-fold increase in FGF-21 mRNA levels was observed. When combined with lithium, there was a 15-fold increase; when combined with VPA, there was a 19-fold increase, and when combined with both lithium and VPA, there was a 50-fold increase (Fig. 2c). The transduction efficiency of lentivirus-mediated control shRNA containing a gene encoding green fluorescence protein (GFP) was estimated to be about 50% in CGCs (Supplementary Fig. S4a & b). We also assessed the effects GSK-3α knock-down on FGF-21 mRNA levels. When a specific sh-GSK-3α construct (#595) was transduced into CGCs via lentivirus to knockdown GSK-3α by about 50%, a relatively small increase in FGF-21 mRNA level was observed either in the absence or presence of lithium or VPA, while a nearly 20-fold increase was observed with GSK-3α shRNA used in the presence of both lithium and VPA, compared with about a 12-fold increase induced by lithium-VPA co-treatment (Supplementary Fig. S4c & d).

Interestingly, augmenting FGF-21 mRNA levels with lithium and VPA was mimicked by co-treatment with lithium and the structurally similar HDAC inhibitors phenyl butyrate (1 mM; PB) or sodium butyrate (1 mM; SB). However, neither PB nor SB alone affected FGF-21 mRNA levels (Fig. 2d), regardless of concentration (Supplementary Fig. S5b). Similar robust effects were observed when the structurally dissimilar HDAC inhibitors vorinostat (1 μM; SAHA) or trichostatin A (100 nM; TSA) were used in conjunction with lithium (Fig. 2e). TSA itself had no effect on FGF-21 mRNA levels (Supplementary Fig. S5c), but SAHA modestly and dose-dependently increased FGF-21 mRNA levels (Supplementary Fig. S5d). MS-275 (5 μM), a class I HDAC-specific inhibitor, also

potentiated lithium's effects. In contrast, the class III HDAC inhibitor nicotinamide (10 mM; Nicotin) had only marginal effects when combined with lithium (Fig. 2f).

Exogenous recombinant FGF-21 protein protects against glutamate-induced excitotoxicity and enhances phosphorylation of Akt-1^{Ser473}, GSK-3β^{Ser9} and ERK 44/42$^{Thr202/Tyr204}$

Next, we examined whether FGF-21 functionally protects against glutamate-induced excitotoxicity in primary neurons. CGCs were treated with 5 μM recombinant FGF-21 protein (PROSPEC Protein Specialists, Rehovot, Israel) at DIV-6, and 100 μM glutamate at DIV-12 for 24 hours. Similar to co-treatment with both lithium and VPA, exogenous recombinant FGF-21 almost completely blocked glutamate-induced neuronal death and chromatin condensation in aging CGCs (Fig. 3a, b). The neuroprotective effects of FGF-21 were associated with a rapid increase in phosphorylation levels of Akt-1^{Ser473} (Fig. 3c), GSK-3β^{Ser9} (Fig. 3d) and ERK 44/42$^{Thr202/Tyr204}$ (Fig. 3e); no changes were observed in total protein levels, indicating activation of Akt-1 and ERK 44/42, and inhibition of GSK-3. Moreover, exogenous FGF-21 blocked glutamate-induced decreases in the phosphorylation of Akt-1, GSK-3β, and ERK 44/42 (Fig. 3f).

To investigate whether lithium-VPA co-treatment affects Akt and GSK-3 activity, CGCs were treated with lithium, VPA, or their combination for different lengths of time, and phosphorylation levels of Akt-1^{Ser473} and GSK-3β^{Ser9} were measured. Lithium alone induced a transient increase in Akt-1^{Ser473} phosphorylation, which returned to baseline within 1–2 hours; VPA alone had no effect (Fig. 4a and c). Notably, co-treatment with lithium and VPA robustly potentiated the lithium-induced Akt-1^{Ser473} phosphorylation, with a detectable increase at 10 min, a maximal response at 2 hours, and a long-lasting 2-fold increase at least 7 days after treatment (Fig. 4a–d). Furthermore, the presence of VPA also potentiated lithium-induced GSK-3β^{Ser9} phosphorylation, while VPA alone had no effect (Supplementary Fig. S6a and b). In addition, levels of phosphorylated ERK 44/42$^{Thr202/Tyr204}$ were modestly increased by lithium-VPA co-treatment (Supplementary Fig. S6c).

FGF-21 is involved in lithium-VPA's neuroprotective effects: the role of Akt-1

Because exogenous FGF-21 activated Akt-1^{Ser473} (Fig. 3c), we next used lentivirus-mediated knockdown of Akt-1 to assess whether Akt-1 also acts as an upstream regulator of FGF-21 expression. CGCs were transduced with five Akt-1 shRNA constructs at the time of plating. Construct #936 was found to be the most effective in reducing total Akt-1 protein levels measured at DIV-6 (Supplementary Fig. S7a). This Akt-1 knockdown was associated with a significant reduction in basal and co-treatment-induced FGF-21 mRNA levels (Fig. 5a, b). Akt-1 knockdown also markedly attenuated the neuroprotection induced by FGF-21 recombinant protein or lithium-VPA co-treatment (Fig. 5c).

To investigate whether FGF-21 expression mediates the synergistic neuroprotection induced by lithium-VPA co-treatment, we transduced CGCs with five constructs of lentivirus-mediated sh-FGF-21. Construct #373 decreased baseline mRNA levels the most (Supplementary Fig. S7b) and lithium-VPA co-treatment-boosted FGF-21 levels (Fig. 5d) by about 50%. In turn, this FGF-21 knockdown markedly decreased phosphorylated

Akt-1^{Ser473} induced by lithium-VPA co-treatment for 2 or 24 hours (Fig. 5e). In addition, sh-FGF-21-induced FGF-21 knockdown blocked co-treatment-induced neuroprotection by about 50% (Fig. 5f).

DISCUSSION

FGF-21 is considered to be a major metabolic regulator targeting the liver, pancreatic islets and adipose tissue to regulate glucose and lipid metabolism[31]. The present study provides the first evidence that FGF-21 is expressed in primary brain neurons. Furthermore, we demonstrated that FGF-21 mRNA and protein expression levels are modestly enhanced by lithium treatment, and remarkably boosted by lithium and VPA co-treatment (Fig. 1). In the case of CGCs co-treated with lithium and VPA, the increase in FGF-21 mRNA levels was synergistic (15–20 fold), persistent (lasting at least seven days), and highly selective among a list of neurotrophic and neuroprotective molecules examined (Fig. 1). It is worth noting that even the closely related FGF family members FGF-15 and 23 were unaffected. This study also demonstrated that the robust induction of FGF-21 mRNA levels by lithium-VPA co-treatment was mediated via GSK-3 and HDAC inhibition, respectively (Fig. 2). Thus, a pharmacological GSK-3 inhibitor SB415 as well as shRNA-mediated GSK-3β knockdown robustly mimicked lithium's ability to up-regulate FGF-21 when used with VPA. Interestingly, lithium in conjunction with SB415 or GSK-3 shRNA also markedly increased FGF-21 mRNA; levels were further increased to 40–50-fold when VPA was present. These potentiating effects of GSK-3 inhibitors or gene silencing likely reflect more severe inhibition of GSK-3 activity due to enhanced serine phosphorylation and decreased tyrosine phosphorylation of this kinase by these treatments [32]. Conversely, VPA's effect on FGF-21 induction in the presence of lithium was mimicked by structurally similar (PB and SB) and dissimilar (SAHA and TSA) pan-HDAC inhibitors. The robust increase in FGF-21 by a class I HDAC-specific inhibitor (MS-275) strongly suggests that class I HDAC isoforms are involved in mediating these effects.

To define the functional role of FGF-21 in primary brain neurons, we demonstrated that exogenous FGF-21 completely blocked glutamate-induced excitotoxicity and apoptosis in aging CGCs, echoing the neuroprotective effects observed with lithium-VPA co-treatment (Fig. 3). Adding FGF-21 also rapidly increased p-Akt-1^{Ser473} levels, as well as its downstream mediator p-GSK-3β^{Ser9}; it also induced a somewhat delayed increase in p-ERK 44/42$^{Thr202/Tyr204}$ levels. Akt is a major cell-survival protein kinase with well-established neuroprotective properties, and its roles in neuroprotection through phosphorylating diverse apoptotic and protective proteins are well documented [22]. It is notable that FGF-21 improves pancreatic β-cell function and survival by activating Akt and ERK, suggesting that FGF-21's insulin-like ability to maintain glucose homeostasis may involve these signaling pathways[33]. As we reported previously, lithium transiently increases p-Akt-1 levels[34]. In this study, we showed that co-treatment with lithium and VPA dramatically prolonged the duration of Akt-1 activation for at least one week (Fig. 4). shRNA-elicited Akt-1 knockdown reduced basal and lithium-VPA co-treatment-induced FGF-21 levels, suggesting that Akt-1 is also an upstream mediator of FGF-21 expression and serves as a feed-forth regulator (Fig. 5). Akt-1 knockdown also attenuated the neuroprotection elicited by exogenous FGF-21 and lithium-VPA co-treatment, further supporting that Akt-1 plays a critical role in protecting against

glutamate excitotoxicity. Importantly, shRNA-mediated silencing of FGF-21 markedly suppressed lithium-VPA-induced neuroprotection from excitotoxicity, suggesting that FGF-21 induction is at least partially responsible for the synergistic protective effects in aging CGCs (Fig. 5). Figure 5g illustrates how Akt-1 is both upstream and downstream of FGF-21, and the manner in which FGF-21 is a critical target for co-treatment with lithium and VPA to induce synergistic neuroprotective effects.

Glutamate-induced excitotoxicity in primary neurons is mediated by overstimulation of NMDA receptors[27]. Growing evidence has linked glutamate excitotoxicity in discrete brain areas to diverse neurodegenerative and neuropsychiatric conditions, including stroke, traumatic brain injury, Huntington's disease, Alzheimer's disease, amyotrophic lateral sclerosis (ALS), spinal cord injury, major depression, and bipolar disorder[21, 22]. In preclinical animal models of ALS, Huntington's disease, and traumatic brain injury, we reported that co-treatment with lithium and VPA was more potent and effective than mono-treatment in inducing neuroprotective molecules, improving behavioral performance, and prolonging life-span[35–37]. Available data set of the expression profile of the human genome indicated that FGF-21 transcript was detectable in the human prefrontal cortex[38] (BrainCloud, braincloud.jhmi.edu). Our study showed that FGF-21 mRNA was induced in the brain of mice after chronic dietary administration with both lithium and VPA, while mono-treatment with either drug was ineffective (Fig. 1f). Further, we provided evidence that FGF-21 can be induced by lithium-VPA co-treatment in rat glioma cells and primary glial cells derived from rat cerebral cortex (Supplementary Fig. S3). Our ongoing studies are investigating whether the pathophysiology of the above-mentioned experimental brain disorders is associated with FGF-21 dysregulation, and whether lithium and VPA combined treatment upregulates FGF-21 expression levels to induce beneficial effects. In this context, two recent studies showed that FGF-21 via acting with its co-receptor β-Klotho on the suprachiasmatic nucleus in mouse hypothalamus regulates brain circadian clock and female reproduction through neuroendocrine control[39, 40], supporting critical neurobiological roles of FGF-21 in the CNS.

It is worth commenting here that the etiology of bipolar disorder is poorly understood. One current working hypothesis is that its pathogenesis involves an interplay between environmental and genetic factors that affect brain plasticity[41]. Although lithium and VPA have been mainstay therapeutic agents for bipolar disorder, only a fraction of individuals with bipolar patients respond to mono-treatment with either drug, and combined lithium and VPA treatment is a rational therapy for these refractory patients[42,43]. Interestingly, patients with bipolar disorder have higher rates of type 2 diabetes mellitus than the general population, and bipolar patients with diabetes have a more severe bipolar disease course and are more resistant to therapy[44]. In light of these clinical observations and our current results, one intriguing possibility that warrants further clinical investigation is that the etiology of bipolar disorder may involve a deficiency in FGF-21 expression levels in the brain and peripheral tissues, and this deficiency might be overcome by lithium and VPA co-administration.

In conclusion, our novel results demonstrate that FGF-21 is expressed in brain neurons, and that its expression levels are boosted by combined treatment with the mood stabilizers

lithium and VPA via the inhibition of GSK-3 and HDACs, respectively. This study also defines a new functional role for FGF-21 in neuroprotection against glutamate-induced excitotoxicity, similar to the effects of lithium and VPA co-treatment. Here, Akt-1 activation acts as an upstream regulator of FGF-21 expression and a downstream mediator for FGF-21-induced neuroprotection. We provide evidence that FGF-21 induction is part of the molecular mechanisms underlying the synergistic neuroprotection induced by mood stabilizers. Our study raises the intriguing possibility that a number of CNS disorders, notably those linked to excitotoxicity, may involve FGF-21 deficiency and that this growth factor could serve as a therapeutic target for certain CNS pathological conditions.

Supplementary Material

Refer to Web version on PubMed Central for supplementary material.

Acknowledgments

This work was supported by the Intramural Research Program of the National Institute of Mental Health, National Institutes of Health (IRP-NIMH-NIH). The authors thank the members of the Molecular Neurobiology Section, NIMH, NIH for their support, and Ioline Henter for critical reading and editing of the manuscript.

References

1. Inagaki T, Dutchak P, Zhao G, Ding X, Gautron L, Parameswara V, et al. Endocrine regulation of the fasting response by PPARalpha-mediated induction of fibroblast growth factor 21. Cell Metab. 2007; 5:415–425. [PubMed: 17550777]
2. Berglund ED, Li CY, Bina HA, Lynes SE, Michael MD, Shanafelt AB, et al. Fibroblast growth factor 21 controls glycemia via regulation of hepatic glucose flux and insulin sensitivity. Endocrinology. 2009; 150:4084–4093. [PubMed: 19470704]
3. Coskun T, Bina HA, Schneider MA, Dunbar JD, Hu CC, Chen Y, et al. Fibroblast growth factor 21 corrects obesity in mice. Endocrinology. 2008; 149:6018–6027. [PubMed: 18687777]
4. Lin WW, Chuang DM. Agonist-induced desensitization of ATP receptor-mediated phosphoinositide turnover in C6 glioma cells: comparison with the negative-feedback regulation by protein kinase C. Neurochem Int. 1993; 23:53–60. [PubMed: 8396484]
5. Xu J, Lloyd DJ, Hale C, Stanislaus S, Chen M, Sivits G, et al. Fibroblast growth factor 21 reverses hepatic steatosis, increases energy expenditure, and improves insulin sensitivity in diet-induced obese mice. Diabetes. 2009; 58:250–259. [PubMed: 18840786]
6. Canto C, Auwerx J. Cell biology. FGF21 takes a fat bite. Science. 2012; 336:675–676. [PubMed: 22582248]
7. Lin WW, Chuang DM. Extracellular ATP stimulates inositol phospholipid turnover and calcium influx in C6 glioma cells. Neurochem Res. 1993; 18:681–687. [PubMed: 8389991]
8. Potthoff MJ, Inagaki T, Satapati S, Ding X, He T, Goetz R, et al. FGF21 induces PGC-1alpha and regulates carbohydrate and fatty acid metabolism during the adaptive starvation response. Proc Natl Acad Sci U S A. 2009; 106:10853–10858. [PubMed: 19541642]
9. Badman MK, Pissios P, Kennedy AR, Koukos G, Flier JS, Maratos-Flier E. Hepatic fibroblast growth factor 21 is regulated by PPARalpha and is a key mediator of hepatic lipid metabolism in ketotic states. Cell Metab. 2007; 5:426–437. [PubMed: 17550778]
10. Muise ES, Azzolina B, Kuo DW, El-Sherbeini M, Tan Y, Yuan X, et al. Adipose fibroblast growth factor 21 is up-regulated by peroxisome proliferator-activated receptor gamma and altered metabolic states. Mol Pharmacol. 2008; 74:403–412. [PubMed: 18467542]
11. Dutchak PA, Katafuchi T, Bookout AL, Choi JH, Yu RT, Mangelsdorf DJ, et al. Fibroblast growth factor-21 regulates PPARgamma activity and the antidiabetic actions of thiazolidinediones. Cell. 2012; 148:556–567. [PubMed: 22304921]

12. Chuang DC, Yeh MC, Wei FC. Intercostal nerve transfer of the musculocutaneous nerve in avulsed brachial plexus injuries: evaluation of 66 patients. J Hand Surg Am. 1992; 17:822–828. [PubMed: 1401789]
13. Li H, Fang Q, Gao F, Fan J, Zhou J, Wang X, et al. Fibroblast growth factor 21 levels are increased in nonalcoholic fatty liver disease patients and are correlated with hepatic triglyceride. J Hepatol. 2010; 53:934–940. [PubMed: 20675007]
14. Belcheva MM, Barg J, Gloeckner C, Gao XM, Chuang DM, Coscia CJ. Antagonist-induced transient down-regulation of delta-opioid receptors in NG108–15 cells. Mol Pharmacol. 1992; 42:445–452. [PubMed: 1328845]
15. Sarruf DA, Thaler JP, Morton GJ, German J, Fischer JD, Ogimoto K, et al. Fibroblast growth factor 21 action in the brain increases energy expenditure and insulin sensitivity in obese rats. Diabetes. 2010; 59:1817–1824. [PubMed: 20357365]
16. Chuang DM, Gao XM, Paul SM. N-methyl-D-aspartate exposure blocks glutamate toxicity in cultured cerebellar granule cells. Mol Pharmacol. 1992; 42:210–216. [PubMed: 1355259]
17. Feingold KR, Grunfeld C, Heuer JG, Gupta A, Cramer M, Zhang T, et al. FGF21 is increased by inflammatory stimuli and protects leptin-deficient ob/ob mice from the toxicity of sepsis. Endocrinology. 2012; 153:2689–2700. [PubMed: 22474187]
18. Planavila A, Redondo I, Hondares E, Vinciguerra M, Munts C, Iglesias R, et al. Fibroblast growth factor 21 protects against cardiac hypertrophy in mice. Nat Commun. 2013; 4:2019. [PubMed: 23771152]
19. Lin WW, Kiang JG, Chuang DM. Pharmacological characterization of endothelin-stimulated phosphoinositide breakdown and cytosolic free Ca2+ rise in rat C6 glioma cells. J Neurosci. 1992; 12:1077–1085. [PubMed: 1312133]
20. Chuang DC, Chen HC, Wei FC, Noordhoff MS. Compound functioning free muscle flap transplantation (lateral half of soleus, fibula, and skin flap). Plast Reconstr Surg. 1992; 89:335–339. [PubMed: 1732905]
21. Chiu CT, Wang Z, Hunsberger JG, Chuang DM. Therapeutic potential of mood stabilizers lithium and valproic acid: beyond bipolar disorder. Pharmacol Rev. 2013; 65:105–142. [PubMed: 23300133]
22. Chiu CT, Chuang DM. Molecular actions and therapeutic potential of lithium in preclinical and clinical studies of CNS disorders. Pharmacol Ther. 2010; 128:281–304. [PubMed: 20705090]
23. Li R, Wing LL, Shen Y, Wyatt RJ, Kirch DG, Chuang DM. Chronic haloperidol treatment attenuates receptor-mediated phosphoinositide turnover in rat brain slices. Neurosci Lett. 1991; 129:81–85. [PubMed: 1656342]
24. Lin WW, Lee CY, Chuang DM. Endothelin- and sarafotoxin-induced phosphoinositide hydrolysis in cultured cerebellar granule cells: biochemical and pharmacological characterization. J Pharmacol Exp Ther. 1991; 257:1053–1061. [PubMed: 1646318]
25. Chuang DM, Leng Y, Marinova Z, Kim HJ, Chiu CT. Multiple roles of HDAC inhibition in neurodegenerative conditions. Trends Neurosci. 2009; 32:591–601. [PubMed: 19775759]
26. Fessler EB, Chibane FL, Wang Z, Chuang DM. Potential Roles of HDAC Inhibitors in Mitigating Ischemia-induced Brain Damage and Facilitating Endogenous Regeneration and Recovery. Curr Pharm Des. 2013; 19:5105–5120. [PubMed: 23448466]
27. Nonaka S, Hough CJ, Chuang DM. Chronic lithium treatment robustly protects neurons in the central nervous system against excitotoxicity by inhibiting N-methyl-D-aspartate receptor-mediated calcium influx. Proc Natl Acad Sci U S A. 1998; 95:2642–2647. [PubMed: 9482940]
28. Leng Y, Liang MH, Ren M, Marinova Z, Leeds P, Chuang DM. Synergistic neuroprotective effects of lithium and valproic acid or other histone deacetylase inhibitors in neurons: roles of glycogen synthase kinase-3 inhibition. J Neurosci. 2008; 28:2576–2588. [PubMed: 18322101]
29. Leng Y, Chuang DM. Endogenous alpha-synuclein is induced by valproic acid through histone deacetylase inhibition and participates in neuroprotection against glutamate-induced excitotoxicity. J Neurosci. 2006; 26:7502–7512. [PubMed: 16837598]
30. Omata N, Chiu CT, Moya PR, Leng Y, Wang Z, Hunsberger JG, et al. Lentivirally mediated GSK-3beta silencing in the hippocampal dentate gyrus induces antidepressant-like effects in stressed mice. Int J Neuropsychopharmacol. 2011; 14:711–717. [PubMed: 20604988]

31. Kharitonenkov A, Larsen P. FGF21 reloaded: challenges of a rapidly growing field. Trends Endocrinol Metab. 2011; 22:81–86. [PubMed: 21194964]
32. Liang MH, Chuang DM. Regulation and function of glycogen synthase kinase-3 isoforms in neuronal survival. J Biol Chem. 2007; 282:3904–3917. [PubMed: 17148450]
33. Wente W, Efanov AM, Brenner M, Kharitonenkov A, Koster A, Sandusky GE, et al. Fibroblast growth factor-21 improves pancreatic beta-cell function and survival by activation of extracellular signal-regulated kinase 1/2 and Akt signaling pathways. Diabetes. 2006; 55:2470–2478. [PubMed: 16936195]
34. Chalecka-Franaszek E, Chuang DM. Lithium activates the serine/threonine kinase Akt-1 and suppresses glutamate-induced inhibition of Akt-1 activity in neurons. Proc Natl Acad Sci U S A. 1999; 96:8745–8750. [PubMed: 10411946]
35. Feng HL, Leng Y, Ma CH, Zhang J, Ren M, Chuang DM. Combined lithium and valproate treatment delays disease onset, reduces neurological deficits and prolongs survival in an amyotrophic lateral sclerosis mouse model. Neuroscience. 2008; 155:567–572. [PubMed: 18640245]
36. Chiu CT, Liu G, Leeds P, Chuang DM. Combined treatment with the mood stabilizers lithium and valproate produces multiple beneficial effects in transgenic mouse models of Huntington's disease. Neuropsychopharmacology. 2011; 36:2406–2421. [PubMed: 21796107]
37. Yu F, Wang Z, Tanaka M, Chiu CT, Leeds P, Zhang Y, et al. Posttrauma cotreatment with lithium and valproate: reduction of lesion volume, attenuation of blood-brain barrier disruption, and improvement in motor coordination in mice with traumatic brain injury. J Neurosurg. 2013; 119:766–773. [PubMed: 23848820]
38. Colantuoni C, Lipska BK, Ye T, Hyde TM, Tao R, Leek JT, et al. Temporal dynamics and genetic control of transcription in the human prefrontal cortex. Nature. 2011; 478:519–523. [PubMed: 22031444]
39. Bookout AL, de Groot MH, Owen BM, Lee S, Gautron L, Lawrence HL, et al. FGF21 regulates metabolism and circadian behavior by acting on the nervous system. Nat Med. 2013; 19:1147–1152. [PubMed: 23933984]
40. Owen BM, Bookout AL, Ding X, Lin VY, Atkin SD, Gautron L, et al. FGF21 contributes to neuroendocrine control of female reproduction. Nat Med. 2013; 19:1153–1156. [PubMed: 23933983]
41. Zarate CA Jr, Singh J, Manji HK. Cellular plasticity cascades: targets for the development of novel therapeutics for bipolar disorder. Biol Psychiatry. 2006; 59:1006–1020. [PubMed: 16487491]
42. Zarate CA Jr, Quiroz JA. Combination treatment in bipolar disorder: a review of controlled trials. Bipolar Disord. 2003; 5:217–225. [PubMed: 12780875]
43. Solomon DA, Keitner GI, Ryan CE, Miller IW. Lithium plus valproate as maintenance polypharmacy for patients with bipolar I disorder: a review. J Clin Psychopharmacol. 1998; 18:38–49. [PubMed: 9472841]
44. Calkin CV, Gardner DM, Ransom T, Alda M. The relationship between bipolar disorder and type 2 diabetes: more than just co-morbid disorders. Ann Med. 2013; 45:171–181. [PubMed: 22621171]

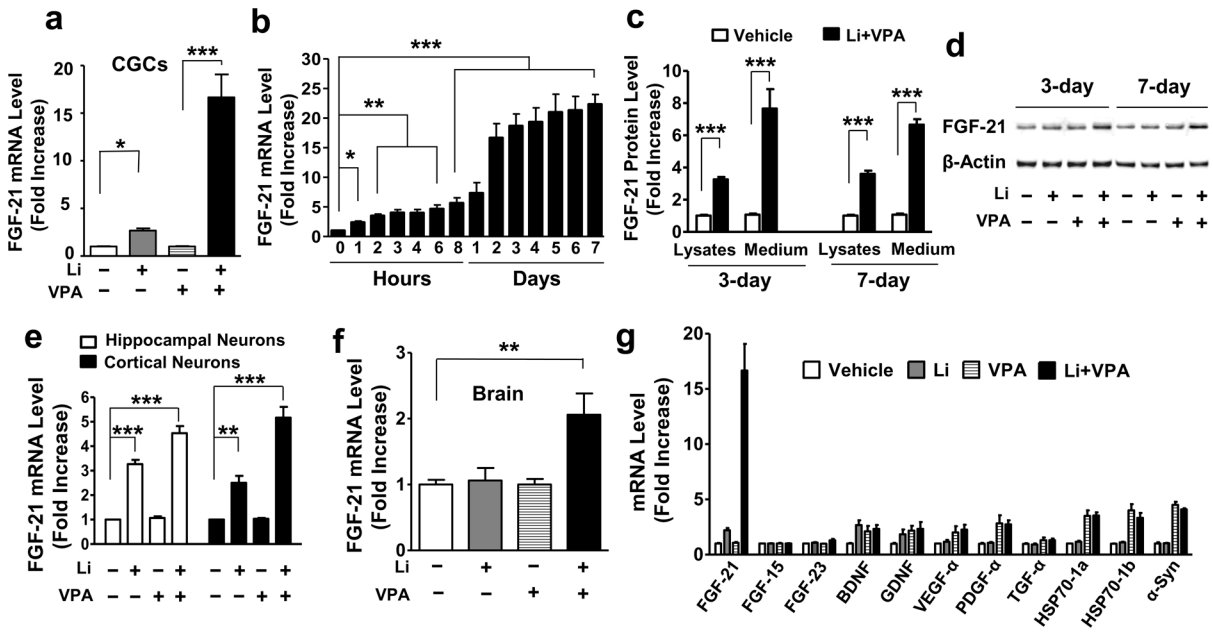

Figure 1. Combined treatment with lithium (Li) and VPA synergistically potentiated FGF-21 mRNA and protein levels in rat primary neurons

(a) CGCs were treated with 3 mM Li, 0.8 mM VPA, or their combination, starting from DIV-6. Two days later, cells were harvested for total RNA extraction, and FGF-21 mRNA levels were detected by q-PCR. **(b)** Starting from DIV-6, CGCs were treated with a combination of 3 mM Li and 0.8 mM VPA for the indicated times, then harvested at DIV-13; FGF-21 mRNA levels were measured by real time q-PCR. **(c)** At DIV-6, CGCs were treated with a combination of 3 mM Li and 0.8 mM VPA. Cell medium and lysates were harvested at DIV-9 or 13 for FGF-21 protein detection using ELISA. **(d)** CGCs at DIV-6 were treated with Li and VPA for 3 or 7 day as described above, then harvested for Western blotting. **(e)** Rat hippocampal and cortical neurons were treated with 2 mM Li, 0.8 mM VPA, or their combination at DIV-6. Cells were harvested 48 hours later for RNA extraction, and real time q-PCR was performed to detect FGF-21 mRNA levels. **(f)** CD-1 mice were fed with diets containing lithium carbonate (3 g/kg), sodium VPA (25 g/kg), or lithium carbonate (3 g/kg)-sodium VPA (25 g/kg) in combination. Four weeks later, whole brains were dissected and used for RNA extraction. FGF-21 mRNA levels, were analyzed by q-PCR. **(g)** CGCs were treated with 3 mM Li, 0.8 mM VPA, or their combination at DIV-6. Two days later, cells were lysed and mRNA levels were measured using q-PCR methodology. Quantified data are means ± SEM and analyzed by one-way ANOVA, n=4–5; *P<0.05; **P<0.01; ***P<0.001.

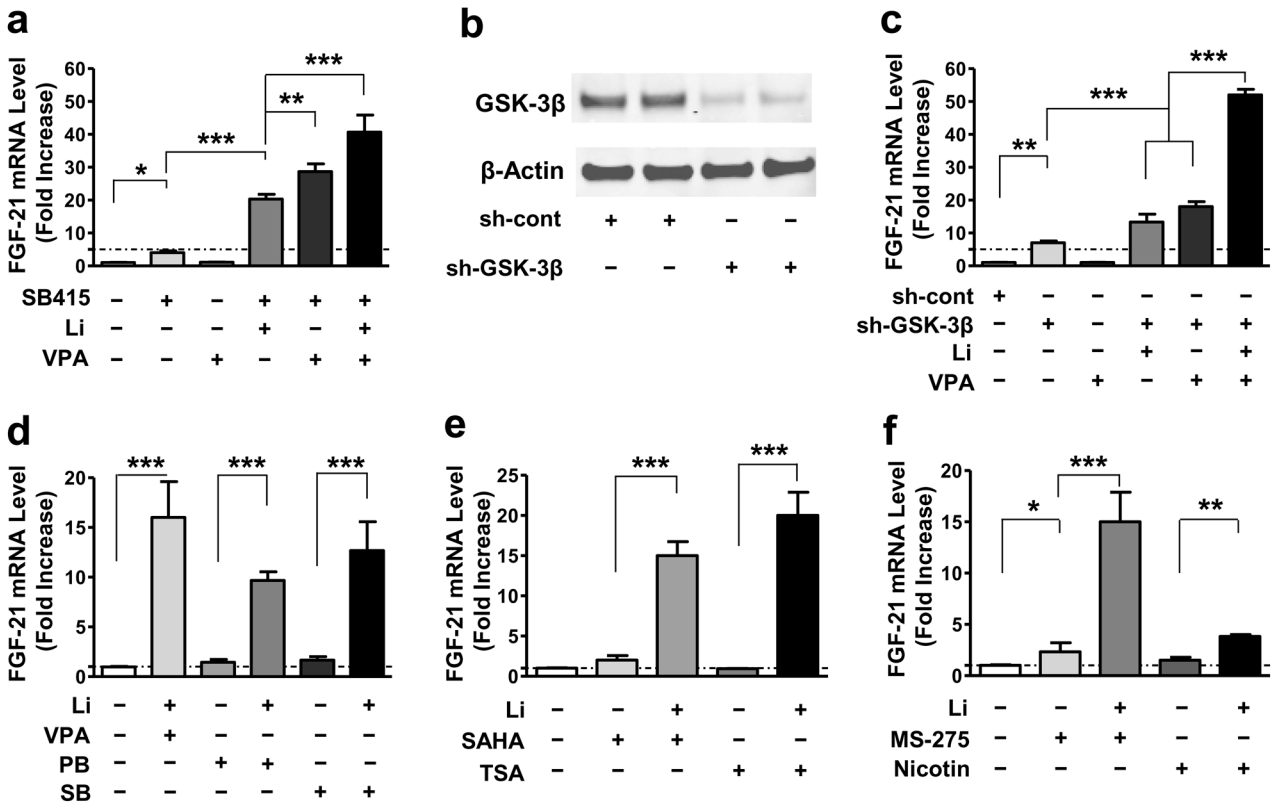

Figure 2. FGF-21 mRNA levels were increased by GSK-3 inhibition, and boosted by a combination of GSK-3 and HDAC inhibition

(a) Starting at DIV-6, CGCs were treated with 10 μM SB415286 (SB415), 0.8 mM VPA, or a combination of 10 μM SB415 with 3 mM Li, 0.8 mM VPA, or with both 3 mM Li and 0.8 mM VPA for 48 hours, then harvested to detect FGF-21 mRNA level by q-PCR. **(b)** CGCs were transduced with sh-GSK-3β (#614) or sh-cont construct at the time of plating. At DIV-6, cells were harvested for Western blotting of total GSK-3β and β-actin protein levels. **(c)** CGCs transduced with sh-cont or sh-GSK-3β were treated with 3 mM Li, 0.8 mM VPA, or their combination, starting at DIV-6. Two days later, cells were harvested and q-PCR was performed to detect FGF-21 mRNA levels. **(d)** CGCs at DIV-6 were treated with 3 mM Li in the absence or presence of 0.8 mM VPA, 1 mM PB, or 1 mM SB. **(e)** CGCs at DIV-6 were treated with 3 mM Li in the absence or presence of 10 μM vorinostat (SAHA), 100 nM trichostatin A (TSA). **(f)** CGCs at DIV-6 were treated with 3 mM Li in the absence or presence of 5 μM MS-275, or 10 mM nicotinamide (Nicotin). The effects of these HDAC inhibitors alone were also assessed. Quantified data are means ± SEM and analyzed by one-way ANOVA, n=3; *P<0.05; **P<0.01; ***P<0.001.

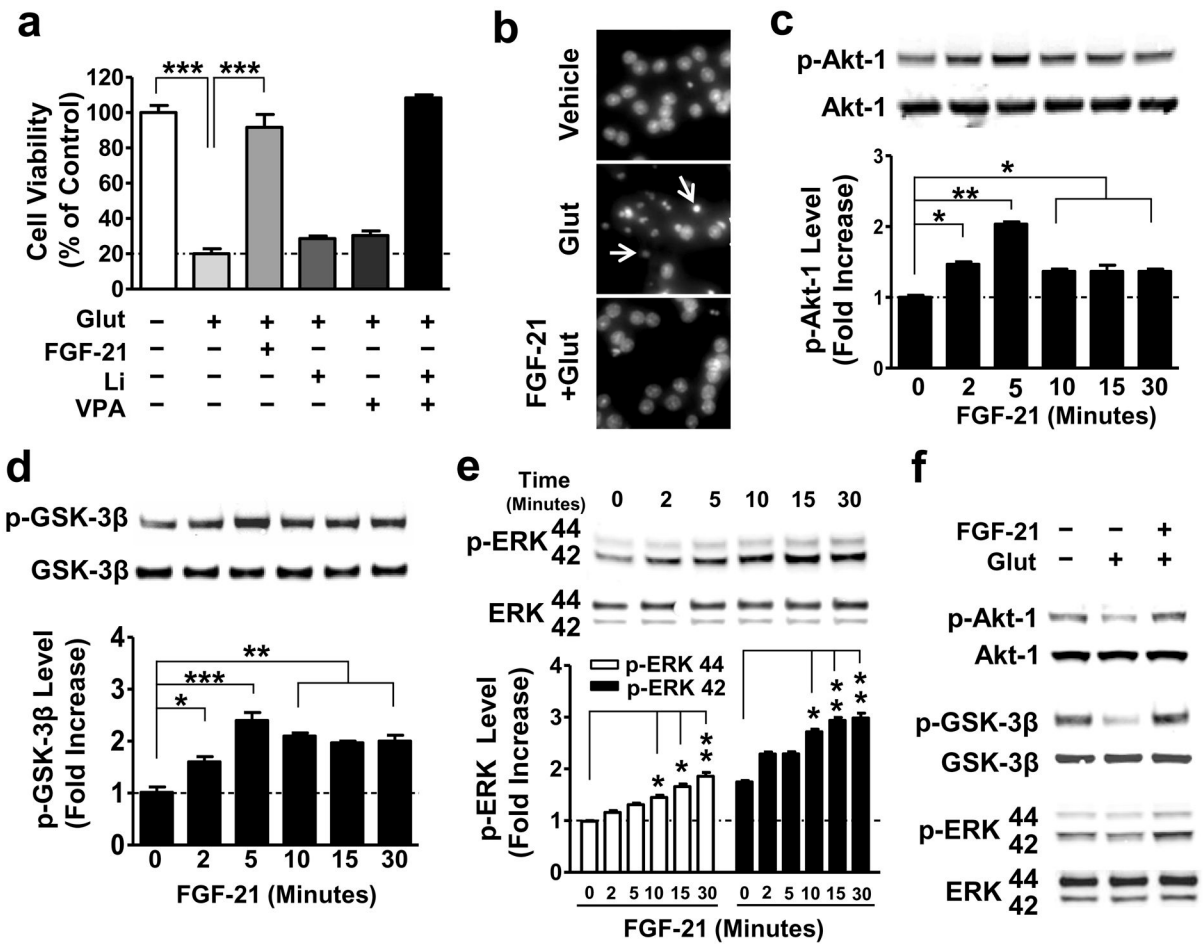

Figure 3. Exogenous FGF-21 protected against glutamate-induced neuronal death, and significantly increased phosphorylation of Akt-1, GSK-3β, and ERK 44/42

(a) CGCs were pre-treated with 5 nM recombinant FGF-21 protein, 3 mM Li, 0.8 mM VPA, or a combination of Li with VPA for 6 days starting at DIV-6. At DIV-12, 100 μM glutamate was added to the culture and cell viability was determined 24 hours later by MTT assay. **(b)** CGCs treated with glutamate with or without FGF-21 pretreatment as described above were also examined for chromatin condensation using Hoechst 33258 staining. Arrows indicate neurons undergoing chromatin condensation. **(c–e)** CGCs were treated with 5 nM recombinant FGF-21 protein for the indicated times at DIV-6, then harvested, and processed for Western blotting to determine levels of p-Akt-1^{Ser473}, p-GSK-3β^{Ser9}, and p-ERK 44/42$^{Thr202/Tyr204}$. **(f)** CGCs were pre-treated with a combination of Li and VPA for 6 days starting at DIV-6, and then treated with glutamate for 6 hours, as described above. Cells were harvested for Western blotting to determine total and phosphorylated proteins of Akt-1^{Ser473}, GSK-3β^{Ser9}, and ERK 44/42$^{Thr202/Tyr204}$. Quantified data are means ± SEM and analyzed by one-way ANOVA, n=4; *P<0.05; **P<0.01; ***P<0.001.

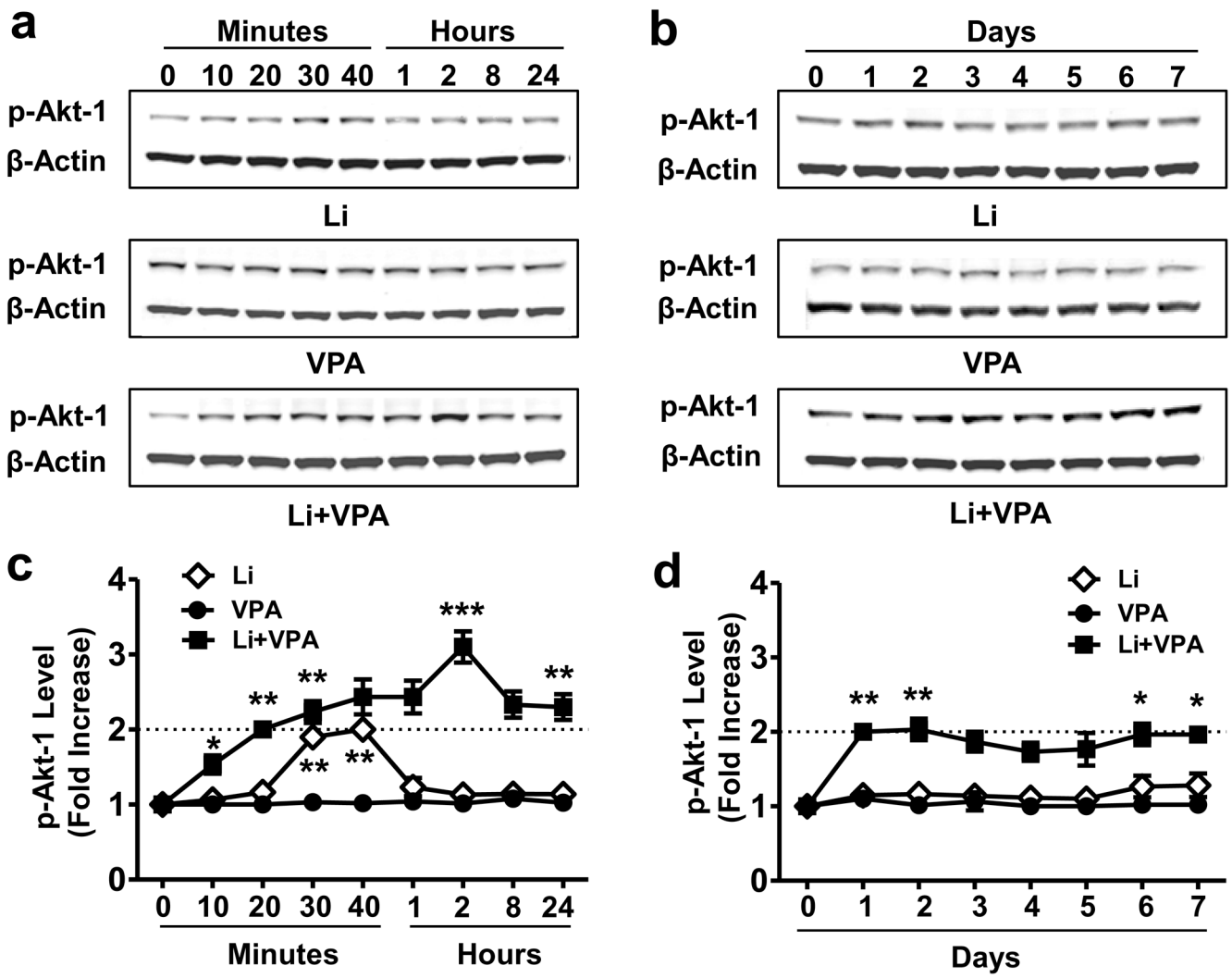

Figure 4. Co-treatment with lithium and VPA dramatically extended lithium-induced Akt-1 activation

CGCs were treated with 3 mM Li, 0.8 mM VPA, or their combination for the indicated times starting at DIV-6, then were harvested at DIV-7 **(a** and **c)** or DIV-13 **(b** and **d)** for Western blotting. Quantified data are means ± SEM and analyzed by one-way ANOVA, n=4; *P<0.05; **P<0.01; ***P<0.001.

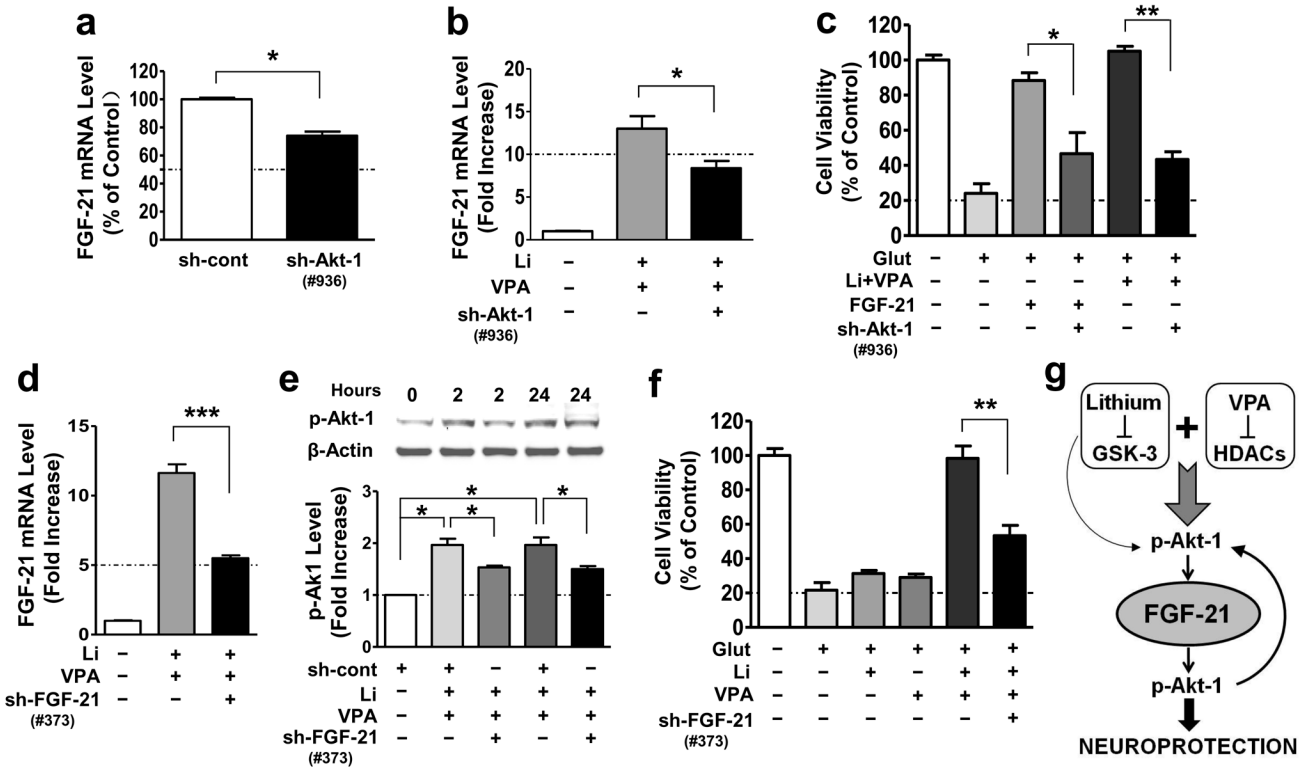

Figure 5. Akt-1 activation and FGF-21 upregulation are required for the neuroprotective effects of FGF-21 and lithium-VPA co-treatment

(a) CGCs were transduced with sh-cont or sh-Akt-1 at the time of cell plating, and harvested for FGF-21 mRNA levels at DIV-6 (n=3, two tailed unpaired *t*-test). **(b)** CGCs were transduced with sh-Akt-1 as described above and then treated with Li-VPA at DIV-6 and harvested at DIV-8 for FGF-21 mRNA detection using q-PCR analysis (n=4, two-tailed unpaired *t*-test). **(c)** CGCs at DIV-6 were treated with 5 nM FGF-21 recombinant protein, or a combination of 3 mM Li and 0.8 mM VPA, followed by exposure to 100 μM glutamate at DIV-12 for 24 hours. Cell viability was determined by MTT assay at DIV-13 (n=3, one-way ANOVA). **(d)** CGCs were transduced with sh-cont or sh-FGF-21 construct at the time of cell plating, and co-treated with 3 mM Li and 0.8 mM VPA at DIV-6, then harvested for q-PCR assay of FGF-21 mRNA levels at DIV-8 (n=4, two-tailed unpaired *t*-test). **(e)** CGCs transduced with sh-cont or sh-FGF-21 as described were co-treated with 3 mM Li and 0.8 mM VPA starting from DIV-6, followed by Western blotting analysis (n=3, one-way ANOVA). **(f)** At DIV-6, CGCs were treated with 3 mM Li, 0.8 mM VPA, or their combination for 6 days followed by exposure to glutamate for 24 hours. Cell viability was determined at DIV-13 using MTT assay (n=3, two-tailed unpaired *t*-test). **(g)** FGF-21 was selectively and robustly induced in aging primary brain neurons by lithium-VPA co-treatment through inhibition of GSK-3 and HDACs, respectively. Lithium and VPA co-treatment induces long-lasting activation of Akt-1 via increased Ser 473 phosphorylation, and this Akt-1 activation is involved in FGF-21 gene expression. Lithium alone only transiently activates Akt-1 and modestly elevates FGF-21 mRNA levels, while VPA alone is ineffective. FGF-21 completely protects primary neurons from glutamate induced excitotoxicity and apoptosis, and these protective effects in return require FGF-21-induced

Akt-1 activation. Thus, Akt-1 serves as a feed-forth regulator for the upstream and downstream actions of FGF-21. FGF-21 induction contributes, at least in part, to the synergistic neuroprotective effects of lithium-VPA co-treatment in aging neurons. Quantified data are means ± SEM; *P<0.05; **P<0.01; ***P<0.001.